Total, Partial, and Electron-Capture Cross Sections for Ionization of Water Vapor by 20–150 keV Protons

F. Gobet, B. Farizon, M. Farizon, and M. J. Gaillard
Institut de Physique Nucléaire de Lyon, IN2P3-CNRS et Université Claude Bernard Lyon 1, 43 boulevard du 11 Novembre 1918, F-69622 Villeurbanne Cedex, France

M. Carré
Laboratoire de Spectrométrie Ionique et Moléculaire, CNRS et Université Claude Bernard Lyon 1, 43 boulevard du 11 Novembre 1918, F-69622 Villeurbanne Cedex, France

M. Lezius, P. Scheier, and T. D. Märk
Institut für Ionenphysik, Leopold Franzens Universität, Technikerstrasse 25, A-6020 Innsbruck, Austria
(Received 23 October 2000)

We present experimental results for proton ionization of water molecules based on a novel event by event analysis of the different ions produced (and lost). We are able to obtain mass analyzed product ion signals (e.g., H_2O^+, OH^+, O^+, O^{++}, H^+) in coincidence with the projectile analyzed after the collision, i.e., either being H^+, neutral H after single electron capture during the ionization event, or H^- after double electron capture. After proper calibration we are thus able to determine a complete set of cross sections for the ionization of a molecular target by protons including the total and the partial cross sections and in addition also the direct ionization and the electron capture cross sections.

DOI: 10.1103/PhysRevLett.86.3751 PACS numbers: 34.50.Gb, 34.70.+e, 87.50.–a

The ionization of water molecules represents not only a fundamental example in collision physics [1], but it is also of great interest in several areas of applied physics spanning the range from radiation damage in biological tissues [2] to the chemistry of the upper planetary atmospheres [3]. Today it is recognized that radiation damage in biomolecules, in particular strand breaking in the DNA, is not only the result of a single interaction of the primary ionization projectile with the molecules involved, but also due to the simultaneous and consecutive action of the primary and the secondary species, including also radicals (for instance oxygen) that are produced by destruction of the water molecules surrounding the DNA. A detailed knowledge of the ionization process is a must for a full understanding of radiation damage on a microscopic level [4].

In spite of the broad range of interest, cross section measurements concerning water are scarce and a number of details have not been investigated up to now. Most studies so far have been restricted to electron impact ionization [5], whereas cross sections for the ionization of water by ion impact are extremely rare. In 1968 Toburen *et al.* [6] reported the first total electron capture cross sections for protons in H_2O in the energy range 100–2500 keV followed by studies about doubly differential ionization cross sections for protons [7,8] and for He^+ and He^{++} ions [9]. These experiments were followed in 1985 by a study of Rudd *et al.* [10] providing absolute total cross sections for proton ionization of water vapor from 7–4000 keV.

More recently, Lutz and coworkers [11] have reported for the first time the investigation of multiple ionization and fragmentation of water after 100–400 keV proton impact, using a position and time-sensitive multiparticle detector. Besides total and partial single ionization, as well as multiple ionization and fragmentation cross sections, their data contain information on the kinetic energy release and the angular correlation for each individual impact event. However, their specialized setup was only sensitive to positive ions produced from water. In particular, they could not detect neutralized projectiles and thus obtain the important information on individual electron-capture cross sections. Despite numerous studies on total capture cross sections for incident protons in various gases [12–14], today there still do not exist any results on partial electron capture cross sections.

In this Letter we report on the application of an experimental setup which allows us, on an event by event basis, to analyze in great detail proton impact ionization of water vapor and to measure partial and total single ionization cross sections as a function of the charge state of the projectile after the ionization event. We are able to obtain mass analyzed product ion signals (e.g., H_2O^+, OH^+, O^+, O^{++}, H^+, and also negative ions) in coincidence with the charge-analyzed projectile, i.e., after the ionizing collision the proton can either be a H^+, a neutral H after single electron capture during the ionization event, or H^- after double electron capture. The present study became possible after the addition of a time of flight mass spectrometer operated in coincidence with our existing high energy ion beam/multicoincidence apparatus [15,16]. In contrast to the earlier correlation experiment by Lutz and coworkers [11] we are now able to analyze the fate of the projectile in coincidence with the fate of the target molecule. For the first time it is possible to provide ionization and

dissociation cross sections that are "differential" in terms of the projectile state.

The experimental setup used and developed here is shown in Fig. 1. It consists basically of five parts (from left to right): first, a proton ion source based on a standard rf discharge burning in H_2 [17]. Second, the ion accelerator allowing us to produce 20–150 keV protons with an energy resolution $\Delta E/E$ of 0.01 [17]. Third, a sector-field type magnetic mass selector for purification of the projectile ion beam. Fourth, a crossed beam interaction region that is combined with a time of flight mass spectrometer. Fifth, a second (sector-field type magnetic) mass selector combined with a multidetector device using three channeltrons that are located at different positions at the exit of the magnetic analyzer, thus giving us information about the final charge state of the projectile (i.e., protons and H^- ions formed by double electron capture will be deflected and neutralized protons will be undeflected by the magnet). In the crossed beam region the energetic proton beam intersects perpendicularly an effusive beam of water vapor (produced by a capillary gas inlet at ambient temperature). The fulfillment of single collision conditions has been checked by changing the densities of both beams. The parent and fragment ions from produced water are extracted perpendicular to the direction of both the projectile and the target beam, and then mass-to-charge analyzed in a home built time of flight analyzer in coincidence with the signals at the multidetector device. This allows us to record for the first time simultaneously the ions produced in the target region and in coincidence for each single collision event the nature of the projectile after the ionizing collision.

The relative measured individual ion currents for the production of a specific product ion (i.e., H_2O^+, OH^+, O^+, O^{++}, and H^+), that is product ions produced irrespective of the fate of the projectile, have been calibrated absolutely by comparison of the present values at 150 keV with the absolute cross sections at 150 keV proton energy reported by Lutz and coworkers [11]. For energies below 150 keV we use the correction factors (accounting for the slightly different detection efficiencies of our mass spectrometer for ions with different mass and kinetic energy) obtained by this procedure to correct our raw data. We calibrate the sum of these corrected raw data at each collision energy with the absolute total cross sections of Rudd *et al.* [10]. This allows us to account for possible different target densities used at the different energies. After this calibration procedure we obtain absolute "partial" cross section curves for the various product ions in the energy range from 20 to 150 keV. Typical examples are shown in the upper part of Fig. 2 exhibiting the data for the production of H_2O^+ and H^+. It should be noted that our present results are smoothly extending the high energy data (100–350 keV) of Lutz *et al.* (which are not shown in these figures for the sake of clarity) to lower projectile energies. This is all the more significant as the partial cross sections have quite different shapes. Whereas the cross section for the production of H_2O^+ is—in a similar manner as the total cross section—monotonously decreasing with increasing energy, the partial cross sections for the fragment ions show a more and more bell shaped form when going from H^+ to OH^+, O^+, and O^{++}, with a maximum cross section positioned at around 25 keV for H^+ and OH^+, 40 keV for O^+, and 50 keV for O^{++}.

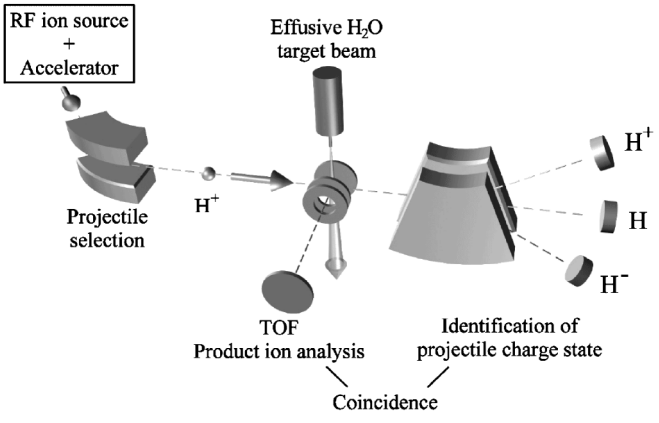

FIG. 1. Schematic view of the experimental apparatus.

More importantly, however, Fig. 2 also shows in the upper part absolute cross sections for ionizing reactions where the projectile remains a proton ("direct" ionization cross section, σ_{di}) and reactions where the projectile recombines via electron capture to a neutral hydrogen atom (capture cross section, σ_c). These differential cross sections (differential in terms of the projectile charge state after the ionizing collision) can be given here for the first time because we have measured in coincidence for each single collision event the identity of the projectile after the ionizing reaction. Except for two data points in this energy regime by Toburen *et al.* [6] and an earlier estimate for the total capture cross sections reported by Rudd *et al.* [10], there exist no earlier data for these cross sections (in particular, concerning the partial cross sections for the individual ions) with which we can compare our results.

An important result from the present investigations is the fact that the two differential cross section curves (that is the "direct ionization" cross section, σ_{di}, and the capture cross section, σ_c) have a strongly different shape. This difference is roughly the same in all cases (i.e., for the total cross sections, $\sigma_{t,di}$ and $\sigma_{t,c}$ as well as for the partial cross sections, $\sigma_{p,di}$ and $\sigma_{p,c}$, two of which are displayed in Fig. 2): the absolute capture cross section is first slightly increasing when going from 20 to 25 keV (reaching at around 25 keV an absolute maximum) and then strongly dropping by almost 2 orders of magnitude when reaching a proton energy of 150 keV. Conversely, the cross section for those events without a change of the projectile charge is slightly decreasing when going from 20 to 30 keV (reaching at around 30 keV an absolute minimum) and then increasing

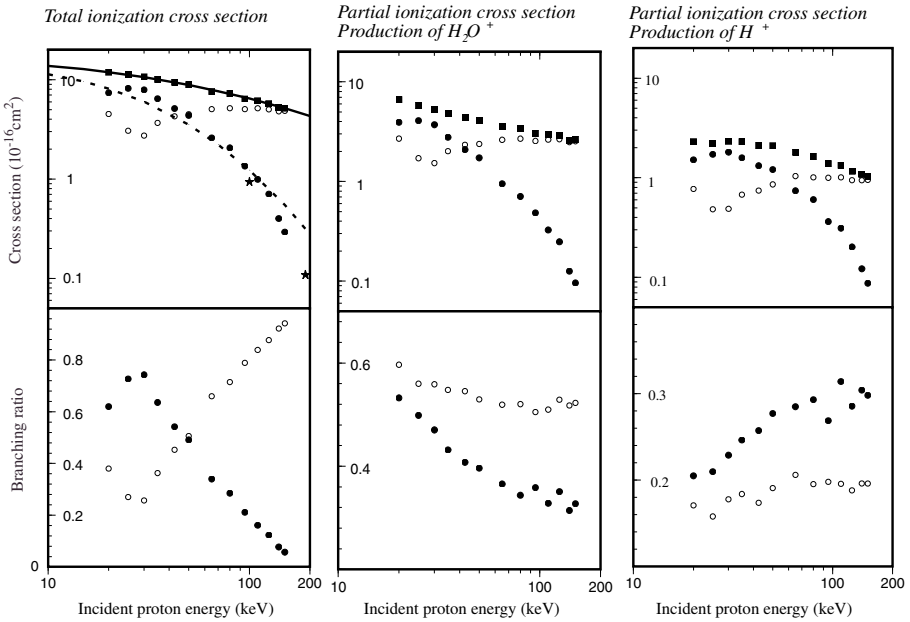

FIG. 2. Upper left panel: Absolute total ionization cross sections for the ionization of H_2O by protons. Present results designated by solid squares, also shown as a solid line for comparison with the data reported by Rudd *et al.* [10] which are in excellent agreement with the results of Lutz and coworkers [11]. In addition, points designated by solid circles represent our results for the total capture cross section σ_c (earlier estimates for this cross section by Rudd *et al.* [10] are shown as a dashed line and two earlier cross section values in this energy range by Toburen *et al.* [6] designated by solid stars) and points designated by open circles total direct ionization (without electron capture) cross section σ_{di}. Upper middle panel: Absolute partial ionization cross sections for the production of H_2O^+ by proton ionization of H_2O. Present results designated by solid squares. In addition, points designated by solid circles represent our results for the partial capture cross section $\sigma_c(H_2O^+)$ and points designated by open circles for the partial direct ionization (without electron capture) cross section $\sigma_{\rm di}(H_2O^+)$. Upper right panel: Absolute partial ionization cross sections for the production of H^+ by proton ionization of H_2O. Present results designated by solid squares. In addition, points designated by solid circles represent our results for the partial capture cross section $\sigma_c(H^+)$ and points designated by open circles partial direct ionization (without electron capture) cross section $\sigma_{\rm di}(H^+)$. In the lower left panel branching ratio $\sigma_c/(\sigma_{\rm di} + \sigma_c)$ is designated by solid circles and $\sigma_{\rm di}/(\sigma_{\rm di} + \sigma_c)$ by open circles. In the lower middle and lower right panels the modified branching ratio $r_p(H_2O^+) = \sigma_p(H_2O^+)/\sigma_c$ and $r_p(H^+) = \sigma_p(H^+)/\sigma_t$, respectively, for electron capture reactions is designated by solid circles and direct ionization reactions (without electron capture) are designated by open circles.

again to the original magnitude reaching a kind of plateau value at around 100 keV. As the absolute values of the two differential cross sections are varying in more or less opposite ways, we can conclude that these two channels are operating in a direct competition to each other, the outcome of this competition depending on the projectile energy.

A deeper insight into the details of this collisional ionization process can be obtained by plotting the branching ratio r for the total cross sections σ_t defined here as $\sigma_{t,di}/(\sigma_{t,di} + \sigma_{t,c})$ and $\sigma_{t,c}/(\sigma_{t,di} + \sigma_{t,c})$, respectively. It is evident that there exists an extremely strong energy dependence of this ratio (see lower part in Fig. 2). Clearly visible is a crossing point with $r = 0.5$ at a proton collision energy of slightly below 50 keV, above this crossing point the probability for electron capture is continuously decreasing in relative importance, finally reaching a probability of about 5% at an energy of 150 keV. Below this crossing point the relative importance of the two channels is first diverging with decreasing collision energy reaching at about 30 keV a maximum in difference (i.e., at this energy the capture cross section is the dominating one with a relative share of about 75%) and below 30 keV with further decreasing energy the two channels are again approaching the same relative magnitude. It is interesting to note that the behavior below the crossing point at about 50 keV is different from what one would deduce from the estimated capture cross sections of Rudd *et al.* [10]. Obviously, such an estimate is very crude and cannot reveal the details which can be obtained when these differential cross sections are measured directly. Moreover, it is quite interesting to note that the branching ratio for the capture cross section reaches its maximum at an incident proton energy of about 30 keV, which is very close to the energy of the proton moving with the Bohr velocity, i.e., 25 keV. Apparently, under this condition electron transfer reaches its highest probability when it is compared to the direct ionization channel.

Partial branching ratios r_p for the individual ions allow us to obtain further insight concerning the fragmentation reaction mechanism. In the lower part of Fig. 2 we have plotted separately for the direct ionization case and the electron capture case the ratio between the respective partial cross section, $\sigma_{p,di}$, or $\sigma_{p,c}$, of the ion under interest divided by the respective total cross section $\sigma_{t,di}$ or

$\sigma_{t,c}$, e.g., for the production of H_2O^+ via direct ionization $r_{p,di}(H_2O^+) = \sigma_{p,di}(H_2O^+)/\sigma_{t,di}$. These plots show a surprising result: the partial branching ratio r_p for the production of the parent ion H_2O^+ via direct ionization is always larger than via electron capture, whereas for the production of the fragment ions (as an example we show the data for H^+ production in Fig. 2) r_p for direct ionization is in almost all cases smaller than for electron capture. Only for the production of O^+ and O^{++} at relatively low collision energy is r_p for direct ionization larger than for electron capture. Moreover, the partial branching ratio r_p for the production of the parent ion H_2O^+ is decreasing with increasing collision energy for both channels, whereas for the production of the fragment ions r_p is increasing with increasing collision energy. Such a reversal (or change) of the relative importance of the two channels when going from the parent ion production to the fragment ion production and when changing the collision energy can be related to the different nature, different energy requirement, and different electronic states involved in producing a parent ion and producing a fragment ion.

In conclusion, we have presented here the first results on an event by event basis for the proton ionization of water vapor. This allows us to obtain a complete analysis in terms of the positive ions in the exit channel. This experiment was possible after combining our high energy ion beam/multicoincidence apparatus with a time of flight mass spectrometer operated in coincidence with the projectile detection. To the best of our knowledge, this is the first time that a complete set of cross sections for the ionization of a molecular target by proton impact has been obtained, including the total and all partial cross sections, and, in addition, differentiating between the direct ionization and the electron capture mechanism.

Work partially supported by the FWF, Wien, Austria and by the Amadee program of the French and Austrian governments.

[1] E. W. McDaniel, J. B. A. Mitchell, and M. E. Rudd, *Atomic Collisions* (Wiley, New York, 1993).
[2] See Proceedings of Molecules of Biological Interest in the Gas Phase, Experimental Tools and Quantum Chemistry EuroConference, Euresco Conference, Centre de Physique des Houches, France, 2000 (unpublished).
[3] C. S. Enos, A. R. Lee, and A. G. Brenton, Int. J. Mass Spectrom. Ion Process **104**, 137 (1991).
[4] B. Boudaiffa, P. Cloutier, D. Hunting, M. A. Hues, and L. Sanche, Science **287**, 1658 (2000).
[5] V. Tarnovsky, H. Deutsch, and K. Becker, J. Chem. Phys. **109**, 932 (1998).
[6] L. H. Toburen, M. Y. Nakai, and R. A. Langley, Phys. Rev. **171**, 114 (1968).
[7] L. H. Toburen and W. E. Wilson, J. Chem. Phys. **66**, 5202 (1977).
[8] M. A. Bolorizadeh and M. E. Rudd, Phys. Rev. A **33**, 888 (1986).
[9] L. H. Toburen, W. E. Wilson, and R. J. Popowich, Radiat. Res. **82**, 27 (1980).
[10] M. E. Rudd, T. V. Goffe, R. D. DuBois, and L. H. Toburen, Phys. Rev. A **31**, 492 (1985).
[11] U. Werner, K. Beckord, J. Becker, and H. O. Lutz, Phys. Rev. Lett. **74**, 1962 (1995).
[12] H. Tawara and A. Russek, Rev. Mod. Phys. **45**, 178 (1973).
[13] L. H. Toburen, IAEA-TECDOC **799**, 47 (1995).
[14] H. Knudsen *et al.,* J. Phys. B **28**, 3569 (1995).
[15] B. Farizon *et al.,* Int. J. Mass Spectrom. Ion Process **164**, 225 (1997).
[16] B. Farizon *et al.,* Phys. Rev. Lett. **81**, 4108 (1998).
[17] M. Carre *et al.,* Mol. Phys. **40**, 1453 (1980).